Quantifying Release of Nano- and Advanced Materials: Determining a Lower Detection Limit

J. Brame[*], A. Poda[*], E. Alberts[**], C. Jackson[*,***], and A.J. Kennedy[*]

[*]US Army Engineer Research and Development Center, Environmental Laboratory, 3909 Halls Ferry Rd. Vicksburg, MS, USA, Jonathan.A.Brame@usace.army.mil
[**]HX5 LLC, 212 Eglin Pkwy. Ft Walton beach, FL, USA
[***]Alcorn State University, Department of Chemistry, Lorman, MS, USA

ABSTRACT

The same unique properties of Manufactured Nanomaterials (MNs) and Advanced Materials (AdM) that make them desirable for new product applications may also increase their environmental health and safety (EHS) uncertainty [1]. Therefore, it is anticipated that MNs/AvMs will have a high risk prioritization under the reformed Toxic Substances Control Act (Frank Lautenberg Chemical Safety for the 21st Century Act) [2], leading to potential delays in production. EHS testing of MNs—and increasingly AvMs—historically began with focus on assessing potential for toxic impacts of pristine materials exposed directly to model organisms, and has since expanded to include more complex environmental matrices and understanding of fate and transport of these materials in the environment [3]. Truly quantifying the risk of these materials requires additional knowledge about how the product is used and the release of MNs/AdMs from the product during use, including any transformations that occur during those releases; however, these release testing processes constitute one of the least understood sources of EHS risk for MN/AdM-enabled products [4], and therefore contribute significantly to the EHS uncertainty. Even incremental improvements in release and exposure quantitation have been encumbered by analytical gaps related to measurement of MN release.

In this report, we show a novel calibration method we have developed to establish a "detection limit" for identification of released NMs (Figure 2). This analysis is the first of its kind, and starts to resolve some of the uncertainty inherent in risk assessment and EHS impacts of MNs/AdMs, particularly in regard to providing some level of confidence in cases where no material is released (i.e., trying to prove a negative).

Keywords: Abrasion, Nanomaterials, Release Testing, environmental health and safety, detection limit, quantification, exposure

1 INTRODUCTION

Nanomaterials are increasingly being used in commercial products to take advantage of nano-specific properties such as strength, electrical and thermal conductivity, anti-microbial capability, optical and fluorescent capacity, and catalytic ability [5]. Although these materials and the products that utilize them hold great potential, that promise is tempered by possible environmental health and safety (EHS) risks of Manufactured Nanomaterials (MNs)[3,6-8]; and as is often the case, regulatory guidance lags technology development. Furthermore, while some EHS hazards exist, they often pose little hazard until the MN is actually released from the matrix within which it is incorporated. In some cases this could be a mixture or liquid dispersion with high release potential, while in other cases materials may be embedded in solid polymer, epoxy or cement-type materials from which the presumed potential for release is substantially lower. Thus it is crucial to understand both the hazard and the exposure to truly quantify the EHS of MNs [9-10].

Several recent studies have attempted to bridge the critical knowledge gap of MN release from nano-composite materials using mechanical abrasion techniques. Release of matrix-bound carbon nanotubes (CNTs) from a nanocomposite required a combination of UV-induced weathering and physical abrasion [11]. Several other studies of general MNs found some level of free, individual release under heavy mechanical stress [12-15], while others found no individual MNs released under similar mechanical stress conditions [16-19]. Many of these studies identified difficulty in generating reproducible results during these mechanical abrasion studies [13,18-19] due to variability in material, abrasion and aerosol sampling as a significant issue in determining release of ENMs. Even when nano-sized particles are identified in a particle size distribution, it can be difficult to determine if they are the ENMs included in a composite formulation or simply small particles of the composite matrix released during abrasion [20,21].

These issues highlight an important need for increased system characterization techniques during mechanical release studies. While some authors provide detailed descriptions of quantification procedures and detection limits for MNs in recovered powders [11], in situ particle measurement techniques such as condensation particle counters (CPS), fast mobility particle sizers (FMPS) and impact particle collectors (IPCs) are rarely characterized for sensitivity and detection limits beyond nominal manufacturer values. In this proceeding we describe a procedure to characterize the lower detection limit for particle concentration (#/cm^3) during MN release testing

using a modified Venturi injection system and a carrier material. The data presented here shows the capability of the method for identifying micro-gram quantities of MNs. Only a small fraction of the MNs in a nanocomposite are likely to be released during mechanical stress, therefore the ability to positively identify such small quantities in situ is crucial for ENM release testing.

2 MATERIALS AND METHODS

2.1 Abrasion Chamber

The abrasion chamber system used in this study is shown schematically in Figure 1. While the chamber is designed to monitor MN release during abrasion, in this study it is utilized for MNs directly injected into the system. Air introduced into the chamber is filtered with a HEPA filter to reduce background particle counts. Air is continuously sampled from the chamber through a sampling port that feeds into an impaction chamber to remove particles >10µm. Then air is passed through a 4-way splitter to a CPC (TSI instruments), a FMPS (TSI instruments) and two filters to collect material for SEM/TEM analysis. Total air flow through the system is 20 LPM (10 LPM for FMPS, 1 LPM for CPC, 4.5 LPM each for the filters). During abrasion tests, a rotating sample platform is positioned under a movable abrasion arm that can be fitted with different abrasive materials (e.g., sandpaper). The abrasion arm has a platform to allow the addition of weights for additional abrasion force. The system was designed as a modification of the standard Taber abrader, used for ISO 7784-2:1997; ISO 9352:1995; ISO 5470-1:1999; and ASTM G195-08.

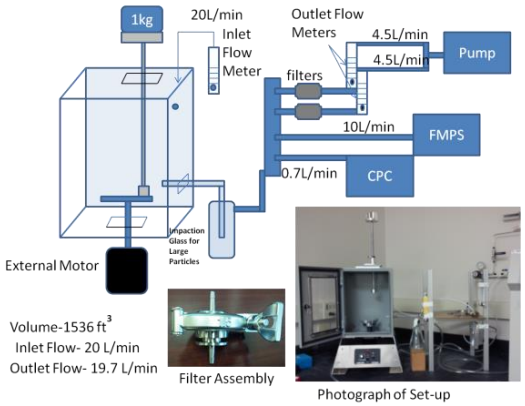

Figure 1: Schematic and photographic representation of the abrasion chamber setup

2.2 Materials

The test material for this study was titanium dioxide (TiO_2) nanomaterial (NIST standard reference material 1898) that is composed of 76% anatase and 24% rutile phase TiO_2, with average primary particle size of 19 ± 2nm and 37 ± 6nm respectively and an overall surface are of 55.55 ± 0.70 m^2/g (NIST certificate). To enable injection of small quantities of TiO_2 into the chamber, a large-scale carrier material was required. The carrier material was a 3-8 mesh silica gel desiccant (Fisher Scientific) that was dried in an oven at 100°C for >2 h and then further sieved to remove any particles smaller than 750 µm. Several dilutions of TiO_2 were loaded onto the desiccant carrier by mixing a controlled mass of TiO_2 into a large quantity of desiccant in a tumbler overnight for distribution on the carrier material. The dilutions used for the study are shown in Table 1.

Material	Test 1	Test 2	Test 3	Test 4
TiO_2 (mg)	10	10	10	100
Desiccant (mg)	20,000	8,000	4,000	4,000
TiO_2/desiccant	0.0005	0.0013	0.0025	0.025

Table 1: TiO_2/Dessicant dilutions used in this study. The study assumes a consistent distribution of TiO_2 on the desiccant carrier.

2.3 Injection Apparatus and Method

Injections of TiO_2 alone and loaded onto the carrier were performed in the abrasion chamber using a modified Venturi Injector (Figure 2). Tests were perfomed in sequences of small-medium-large mass ranges (approx 5mg, 10mg, and 20mg for TiO_2 alone). Desiccant carrier samples were also injected in a small-medium-large sequence (approx 50mg, 200mg, 500mg of desiccant). Between each of these sets, the interior of the abrasion chamber, as well as the injecter apparatus and tubing for downstream airflow were cleaned with water and pressureized air to remove residual TiO_2.

For all tests, the sample was weighed and placed in the sample tube (Figure 2), and the entire injector was enclosed within the chamber system. A five minute baseline was recorded prior to injection of the sample to obtain a measurment of the particles present in the air. An injection of N_2 at 120kPa is passed through the Venturi Injector, creating a vacuum in the sample tube and pulling the sample into the injection flow, which is dispersed throughout the chamber. Injection of N_2 was run for five minutes to maximize material removal from the sample tube. After this time, the N_2 flow was shut off and data collection contiued for an additional five mintues to record the post-test return to baseline.

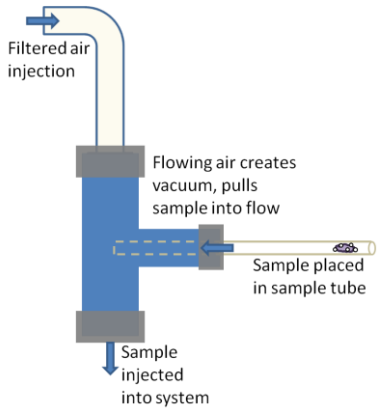

Figure 2: Schematic representation of the injection apparatus

3 RESULTS AND DISCUSSION

FMPS data (Figure 3) show a wide particle size distribution with peak concentration centered at the 143nm size bin of the instrument. This average size was consistent across various masses of TiO_2 injection into the abrasion chamber. When attached to the dessicant carrier, we see a slight shift down to 124nm peak particle size, which in the FMPS is the adjacent size bin. The dessicant carrier alone did not exhibit any significant signal in the FMPS, and can therefore be a useful carrier for most types of NP release testing.

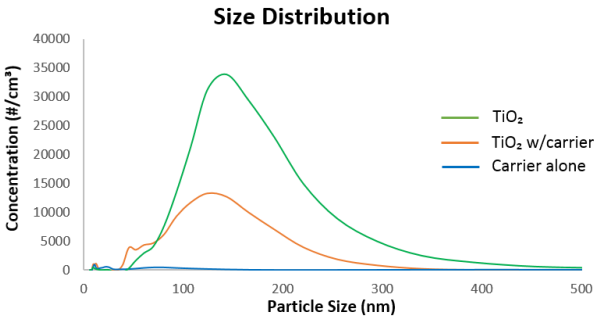

Figure 3: Representative particle distribution for TiO_2 (4mg) alone, TiO_2 with carrier (100mg), and carrier alone (100mg).

Particle size distribution was calculated by averaging the concentration of particles during the entire injection time and subtracting the baseline recorded before the run, to correct for any non-TiO_2 particles in the air detected by the instrument. While these particle size distribution plots can allow us to be selective of which channels to take into account when deriving trends in the data, we did not find significant differences when selected or all channels were used for TiO_2 injection analysis.

For each injection we can approximate the amount of material that passed through the FMPS by integrating the area under the curve in the particle concentration over time plot. In general, we expect that larger mass of TiO_2 injected will yield a larger curve (more particles) and hence a larger area. Plotting this calculated area versus the measured mass for each test yields the scatter plot in Figure 4.

Injections of TiO_2 without dessicant carrier ranged in mass from 3.9mg to 23.3mg. In Figure 4 we see a wide range of calculated areas (within an order of magnitude), even for points of equivalent injected mass. However, as injected mass decreases we see a corresponding decrease in the measured area, as well as a reduction in the data spread. The variance in these measurements is not entirley unexpected, and is likely due to several sources of error.

The most significant error in this plot is the disparity between the measured mass of TiO_2 and the mass that is taken in and recorded by the instrument. The total air flow into the air sampler (20L/min) allows for complete volume exchange over 1-2 minutes, while the peak particle measurement occurs for only a few seconds. After injection, TiO_2 dust can be observed coating the chamber walls and in the injecter apparatus itself.

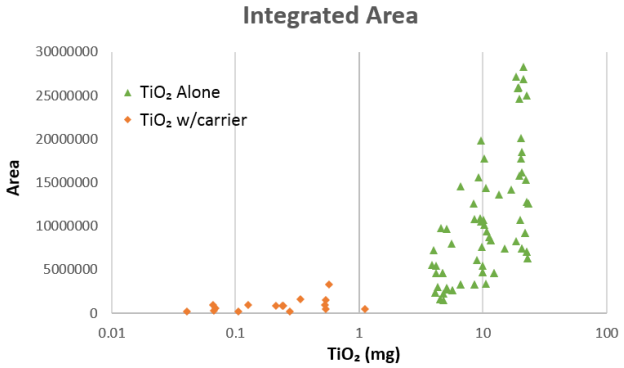

Figure 4: Integrated areas of TiO_2 injections with and without carrier. The calculated areas serve as a representation of how much material passed through the FMPS. TiO_2 mass is plotted on a logarithimc scale

It was anticipated that as the injected mass decreaed, eventually the instrument would no longer be able to detect the particles being injected (area=0). However, when <1.0mg masses were recorded with the carrier trials, the zero area point is never achieved, but instead is approached asymptotically. Previous abrasion tests containing no NPs, as well as the dessicant alone trials, yielded no signal that could be distinguished from background noise. However, any trial that did contain NPs, no matter how small the amount, consistently yielded a signal in the FMPS.

The dessicant carrier experiments have the same issues with error as the TiO_2 alone in that there is a disparity between injected mass and the mass that is recorded by the FMPS, due in part to some of the TiO_2 remaining adsorbed to the dessicant carrier.

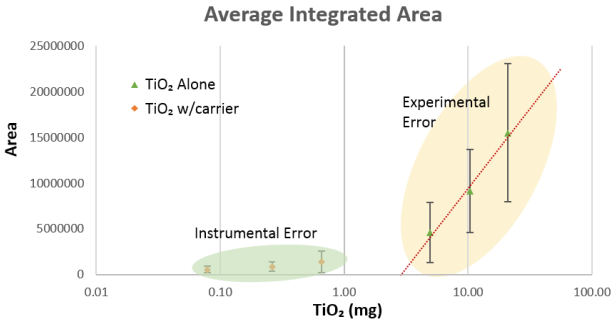

Figure 5: Integrated areas grouped as small, medium, or large injections and averaged. Colored regions define predominantly instrumental and experimental error regions. The mass of TiO_2 is plotted on a logarthimic scale

In Figure 5, the injections have been grouped into their corresponding small, medium, and large trials for the carrier and non-carrier experiments. Averaging these groups provides another way of examining the range in the data as well as further emphasizing the observed aysymptotic trend. From collected data, we can also divide then plot into two regions, the first region (>1.0mg TiO_2 injection) being dominated by experimental error, characterized by large variance in the integrated areas. A logarithmic fit to the yellow-shaded data in Figure 5 indicates a theoretical x-intercept (zero area) near 2 mg injected mass. Mass less than 3-5 mg was experimentally difficult to use via direct injection with this method, and the carrier injection method produced an alternative regime asymptotically approaching zero area. This second region (<1.0mg TiO_2), where we see the data approach but never reach zero, is dominated by instrumental error. Here we are limited by the instrument itself, and it becomes difficult to determine the lower limit of concentration where the FMPS can no longer detect MNs.

Despite the sources of error in this method, it represents a first attempt to evaluate low-limit detection of MN release in abrasion testing. As the quantity of nano particles released during mechanical abrasion is usually unknown, we have determined the capability of the instruments in this method to measure small masses of MNs (0.1-1.0mg). With some understanding of the regions of uncertainy when analyzing the data, we can make better assumptions as to the quantity of material that may be released and the quality of the data generated. The inability to obtain a true zero point in the detection limit makes it difficult to say that no NPs are released from a given sample known to contain NPs even if no apparent signal is detected by the FMPS. Instead this limit will have to be addressed in terms of percent confidence that the quanity of nanoparticles is below a certain concentration or even at zero. These observations must be considered when performing abrasion tests to determine if NP containing materials meet environmental standards. The results and procedure represent an incremental improvement in release quantitation confidence, which will lead to reduced uncertainty when estimating the exposure component in MN risk assessments.

REFERENCES

[1] A. Wardak, et. Al. Journal of Industrial Ecology, 12 (13), 435-448, 2008

[2] TSCA, *The Frank R. Lautenberg Chemical Safety for the 21st Century Act*, EPA, 2016.

[3] G. Oberdorster, E. Oberdorster, and J. Orberdorster. Environmental Health and Perspectives, 113(7), 823-839, 2005

[4] H. Wigger, et al., Science of the Total Environment, 535, 160-171, 2015

[5] J. Brame, O. Li, P. Alvarez, Trends in Food Science and Technology, 22, 618-624, 2011

[6] S. Bakand, A. Hayes, F. Dechsakulthorn, Toxicology, 24, 125-135, 2012

[7] CW. Lam, JT James, R. McCluskey, S. Arepalli, RL. Hunter, Critical Reviews in Toxicology, 36, 189-217, 2006

[8] Y. Liu, YL. Zhao, BY. Sun, CY. Chen, Accounts of Chemical Research, 46, 702-713, 2013

[9] ZA. Collier, et al. J. Nanopart Res 17, 1-21, 2015

[10] S. Frogget, S. Clancy, D. Boverhof, R. Canady, Particle and Fiber Toxicology, 11(17), 1743-8977, 2014

[11] S. Hirth. L. Cena, G. Cox, Z. Tomovic, T. Peters, W. Wohleben, J. Nanopart Res, 15, 1504, 2013

[12] B. Fiorentino, L. Golanski, A. Guiot, JF Damlencourt, J Nanopart Res, 17, 1-13, 2015

[13] L. Golanski, A. Guiot, M. Pras, M. Malarde, F. Tardif, J Nanopart Res, 14, 1-9, 2012

[14] G. Huang, JH. Park, L. Cena, B. Shelton, T. Peters, J. Nanopart Res, 14, 2012

[15] L. Schlagenhauf, BTT Chu, J. Buha, F. Nuesch, J. Wang, Environmental Science & Technology, 46, 7366-7372, 2012

[16] D. Bello, et al., J Nanopart Res, 11, 231-249 (2009)

[17] L. Cena, T. Peters, Journal of Occupational and Cenvironmental Hygiene, 8, 86-92, 2011

[18] D. Gohler, M. Stintz, L. Hillemann, M. Vorbau, Annals of Occupational Hygiene, 54, 615-624, 2010

[19] M. Vorbau, L. Hillemann, M Stintz, Journal of Aerosol Science, 40, 209-217, 2009

[20] H. Dylla, M. Hassan, J Nanopart Res, 14, 1-15, 2012

[21] J. Brame, et al. Environmental Science & Technology, 49 (19), 11245-11246, 2015